

# Accepted Manuscript

A Compilation Of Data On The Radiant Emissivity Of Some Materials At High Temperatures

J.M. Jones, P.E. Mason, A. Williams



PII: S1743-9671(17)31003-6

DOI: [10.1016/j.joei.2018.04.006](https://doi.org/10.1016/j.joei.2018.04.006)

Reference: JOEI 444

To appear in: *Journal of the Energy Institute*

Received Date: 21 December 2017

Revised Date: 19 April 2018

Accepted Date: 23 April 2018

Please cite this article as: J.M Jones, P. Mason, A. Williams, A Compilation Of Data On The Radiant Emissivity Of Some Materials At High Temperatures, *Journal of the Energy Institute* (2018), doi: 10.1016/j.joei.2018.04.006.

This is a PDF file of an unedited manuscript that has been accepted for publication. As a service to our customers we are providing this early version of the manuscript. The manuscript will undergo copyediting, typesetting, and review of the resulting proof before it is published in its final form. Please note that during the production process errors may be discovered which could affect the content, and all legal disclaimers that apply to the journal pertain.

**A COMPILATION OF DATA ON THE RADIANT EMISSIVITY OF SOME MATERIALS AT HIGH TEMPERATURES**

J.M Jones, P E Mason and A. Williams\*

School of Chemical and Process Engineering, The University of Leeds

Leeds, LS2 9JT, UK

\*Corresponding author: fueaw@leeds.ac.uk

**1 ABSTRACT**

2 This paper gives a compilation of experimental data from a variety of sources of the emissivity of  
3 materials used in high temperature applications. The data is given in the form of temperature  
4 dependent correlation equations which can be used for modelling purposes. The data on refractory  
5 materials show the importance of surface properties, the effect of surface coatings and ways in which  
6 these can be taken into account for more accurate predictions of emissivity. Information is also given  
7 on chars, ash particles and furnace deposits resulting from the combustion of coal and biomass.

8 Keywords: emissivity; metals; refractories; chars; ash deposits.

9

## 1. INTRODUCTION

Radiant heat transfer plays an important role in many engineering applications. An accurate knowledge of the emissivity of all the surfaces at high temperatures in a furnace or processing unit is an essential requirement. For all the materials involved the emissivity varies with temperature and spectrally. However, in many modelling applications such as combustion plant, the complexity of the computations may require an average value of total normal emissivity to be used, although the accuracy is improved if the variation with temperature can be included.

Over the last 80 years, the need to have more accurate data on the emissivity of ceramic and metallic solids has mainly been driven by their use for furnace applications in the metallurgical and glass industries. Later developments resulted from the requirements of the space industry, and more recently by CFD modelling of the combustion of coal and biomass by the power industries, for example [1-9]. In these applications details are required of the variation of emissivity with temperature and the nature of the surface. This paper is an updated version of an earlier review [6] for a number of materials of particular interest for high temperature applications.

Whilst extensive compilations of thermal radiative data are available for metals and also non-metallic solids, [7,8] this does not include certain engineering materials such as furnace linings and slags produced as the result of combustion or gasification. The nature and optical properties of the surface may change during use and this is especially the case with materials in high temperature furnaces or fires where metals may become coated with oxide, and in the case where ash may melt or sinter to form surface layers. This problem has been intensified because of the desire to increase the productivity of furnace heating applications by the use of ceramic fibre furnace linings or use of 'high-emissivity' coatings [9]. The advantages of lining furnaces with ceramic fibre materials are usually stated to be that the low thermal mass of the fibre leads to a reduction in the quantity of heat required to bring the furnace up to temperature and, consequently, to shorter heat up times. The relatively high resistance to thermal shock means that the walls can be heated and cooled rapidly without damage, and the low thermal conductivity of the fibre minimises heat loss through the furnace walls. However, when ceramic fibres have been used to line furnaces whose main mode of operation is continuous heating, the actual energy savings have sometimes been lower than expected. It has been suggested that this results from the low emissivity of the ceramic fibres and that increased heat transfer to the stock can be expected if they are coated with a layer of high emissivity refractory. The use of high emissivity coatings, with or without ceramic fibres has been held to be appropriate

because: (i) the high emissivity has been assumed to lead directly to high rates of net heat transfer and (ii) the coatings protect the refractory and prolong its life, and reduce air leakage. In the light of this continuing interest, there is a need for accurate emissivity data for furnace modelling.

The world-wide use of pulverised coal firing for electricity generation, and more recently similar plants using 100% biomass or co-firing with coal, has resulted in extensive modelling studies to improve combustor performance. These combustion systems are complex in that they involve burning particles of the fuel. Accounting for spectral variation in the emissivity of the particles and furnace surfaces adds even more complexity, so for most modelling applications ‘averaged’ values of emissivity data have to be employed [10, 11] or at specific wavelengths [12].

Another important application arises from the wide use of radiation thermometers based on semiconductor infra-red detectors, where the temperature deduced is a function of the assumed emissivity of the surface. To infer accurate measurements, it follows that accurate emissivity data are required. Many manufacturers of non-contact infrared measurement equipment give lists of emissivity data with the cautionary statement that this data is to be used as a guide only, as the value changes dependent on the actual surface and conditions. Such data are given at 1.0, 1.6 and 8-14  $\mu\text{m}$  by, for example, by Fluke Process Industries [13].

## 2. THE DEFINITION OF SURFACE EMISSIVITY

The emissivity of a surface is defined as the ratio of the radiance from the surface to that from a black body viewed under identical optical and geometrical conditions and at the same temperature. The total black body radiation flux density, or emissive power  $E_b(T)$  at a known temperature,  $T$ , is obtained from integration of the black body spectral flux,  $e_b(\lambda, T)$ , over all the wavelengths:

$$E_b(T) = \int_0^{\infty} e_b(\lambda, T) d\lambda \quad (1)$$

This gives:

$$E_b(T) = \sigma T^4 \quad (2)$$

The total temperature dependent emissivity of a surface,  $\varepsilon_t(T)$ , may be written in terms of the black body emissive power and spectral flux density of the surface,  $e(\lambda, T)$ , as:

$$\varepsilon_t(T) = \frac{1}{E_b(T)} e(\lambda, T) d\lambda \quad (3)$$

65 Integration of  $e(\lambda, T)$  over the spectral band limits  $(\lambda_1, \lambda_2)$  will yield the spectral emissivity  $e_{\lambda_j}(T)$ :

$$e_{\lambda_j}(T) = \frac{1}{\Delta E_{b\lambda_j}(T)} \int_{\lambda_1}^{\lambda_2} e(\lambda, T) d\lambda \quad (4)$$

66 where  $\lambda_j$  is the nominal wavelength position which defined by:

$$\lambda_j = (\lambda_1 + \lambda_2)/2 \quad (5)$$

67 and  $\Delta E_{b\lambda_j}(T)$  is the black body band emissive power over the same wavelength range. The way in  
 68 which the emissivity is determined is dependent on the temperature and the spectral range. Thus in  
 69 the major study of total and spectral emissivity of pure metals and specific inorganic compound  
 70 published in '*Thermophysical Properties of Matter*' [7,8], measurements are made over the range of  
 71 1-15  $\mu\text{m}$  with the calibrating black body covering the same spectral range. In later work, especially  
 72 when interest was concentrated on the spectral properties of coal ash, it was found to be more  
 73 accurate to ratio samples to grey body references, for example [14,15]. When a grey body radiator is  
 74 used as the reference, the measured sample emissivity is related to the true emissivity by a  
 75 calibrating function.

76 The total normal emissivity,  $\varepsilon(T)$ , is determined by weighting the spectral emissivity,  $e_{\lambda_j}(T)$ , with  
 77 the Planck function,  $I_b$ , as in Eq. 6 below.

$$\varepsilon(T) = \frac{\int_{\lambda_1}^{\lambda_2} e(\lambda, T) \cdot I_b(\lambda, T) d\lambda}{\int_{\lambda_1}^{\lambda_2} I_b(\lambda, T) d\lambda} \quad (6)$$

78 Since the spectral emissivity is weighted by the Planck function (Planck-weighted) the total normal  
 79 emissivity calculated in this way is slightly different to Eq. (4). This method of calculating the total  
 80 emissivity, for example as used in references [16-18], results in slightly different absolute values,  
 81 although both methods are used in the literature. Application of the Planck correction influences the  
 82 temperature dependency of the total normal emissivity. In the case of metals the effect is very small  
 83 at temperatures up to 1000 K, but at 2000 K it increases the emissivity by about 8 %. However Eq. 6  
 84 is used when spectral emissivities are measured primarily for coal or biomass ash deposits or  
 85 particles, and for heavily oxidised metal surfaces. These inorganic species have a spectral region of

low emissivity at wavelengths up to 2 or 3  $\mu\text{m}$  followed by a region of high emissivity at longer wavelengths, which is usually strongly banded [19,20]. For fuel ashes the use of Eq.5 rather than Eq.4 leads to slightly lower total emissivities but also a slightly different temperature variation..

In the analysis of radiative heat transfer, the definition of emissivity is often used ambiguously. The emissivity of a surface or body is always defined as the ratio of the radiation emitted by the surface to the maximum possible, that is, from a black body at the same temperature. However, since temperature, wavelength and direction may all affect this ratio, they should all be included in a fully comprehensive definition. Arising from this requirement, a number of individual definitions may be encountered in the literature: (i) for radiation from a body at a particular temperature, the directional, monochromatic emissivity relates to radiation at a defined wavelength and direction (usually expressed as an angle,  $\theta$ , to the normal), (ii) if radiation over the whole range of thermal wavelengths but in a specific direction is considered then the appropriate term is the total, directional emissivity, (iii) similarly, if all the radiation emitted at a particular wavelength into the hemisphere beyond the surface is involved, the appropriate definition is that of the monochromatic, hemispherical emissivity.

The value used in many analyses of radiative heat transfer in furnace enclosures is the simplest one. It relates to radiation at all wavelengths and in all directions and is the total, hemispherical emissivity. It is the value used to multiply  $\sigma T^4$  the Stefan-Boltzmann expression, and it is often referred to simply as the emissivity. For real surfaces, the ratio of radiation emitted by the surface to that emitted by a black body at the same temperature is often called the emittance, although the definition is exactly the same as for emissivity for smooth surfaces. In this paper we usually use the term emissivity referring to total normal emissivity rather than emittance, but the latter term is used for non-perfect surfaces such as refractories. Thus depending on the source of information (as is the case in some of the figures here) and since the terms are effectively interchangeable this is adopted here following the approach in previous publications, for example in reference [1]. Indeed most industrial and research workers use it. Some data for total hemispherical emissivity are included in some of the Tables because these values are within about 5% of the total normal emissivity for most real materials as discussed later in the next section.

### 3. EXPERIMENTAL VALUES OF EMISSIVITY

Typical values of emissivity for a tungsten filament [7,21] are shown in **Fig 1** which illustrates the variation of emissivity with both temperature and wavelength for a metal. The variation in

wavelength follows theory for a radiating metal surface. In addition to these factors the emissivity can change if the surface is oxidised or if it is a rough surface. In fact many metals subject to high temperatures in a furnace or fire situation oxidise so they are coated with a metal oxide; the exceptions are the noble metals and to a certain extent some of the stainless steels. Not only does the emissivity change but the spectral properties change too depending on the thickness of the oxide layer. As shown in Fig. 1, metals have a high emissivity at low wavelengths which decrease with wavelength especially at lower temperatures. As discussed earlier, many inorganic oxides behave in the opposite way especially fuel ashes, eg [19,20].

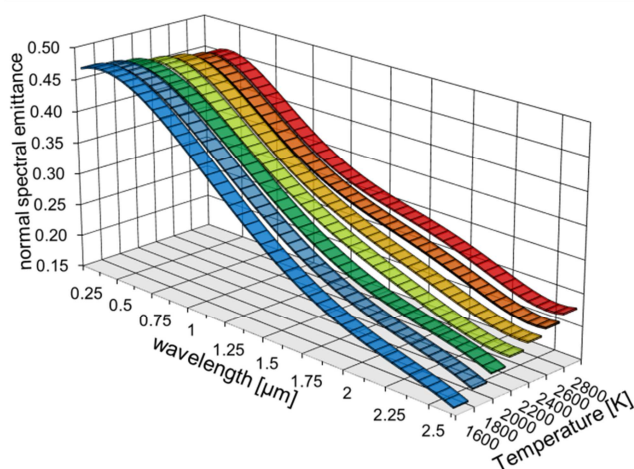


**Fig 1.** Spectral emittance of tungsten. Based on [7, 14].

Non-conducting materials, such as ceramics, have more complex spectral behaviour which can be further complicated by surface roughness and purity effects. **Fig 2 (a)** shows the variation of the emittance with temperature for a pure ceramic, aluminium oxide, and the typical experimental error that can arise which in this case is about  $\pm 0.1$  [8]. The errors that arise can come from measurement of the surface temperature which can have a large influence, but it also depends on whether the emissivity has a strong variation with temperature. In the example in **Fig 2 (a)** this is not the case but variation in surface finish and purity of the sample are important. Instrumental factors such as internal reflectance have to be minimised. **Fig 2 (b)** shows the effect of the purity on the spectral emittance from commercial aluminium oxide [8]. These plots clearly show the scatter that can arise. Different surface finishes and different experimental methodology can have a major influence on reproducible measurements from different laboratories.

The normal emittance curves given in **Fig 2 (b)** are typical for inorganic oxides, but also for fuel ashes [20] where the composition of the ash can markedly vary from fuel to fuel. Another industrially important example of where slight variations in composition can markedly impact on the



spectral emissivities is in the case of Ni and Fe-based boiler tubes in a high temperature oxidising environments. It was found in laboratory experiments [22] that the emissivities of metals containing more than 9 wt% of chromium have the typical behaviour of metals, this resulting from the resistance to oxidation. This is not the case when the Cr content is below 2 wt% when the behaviour become that of an oxide,

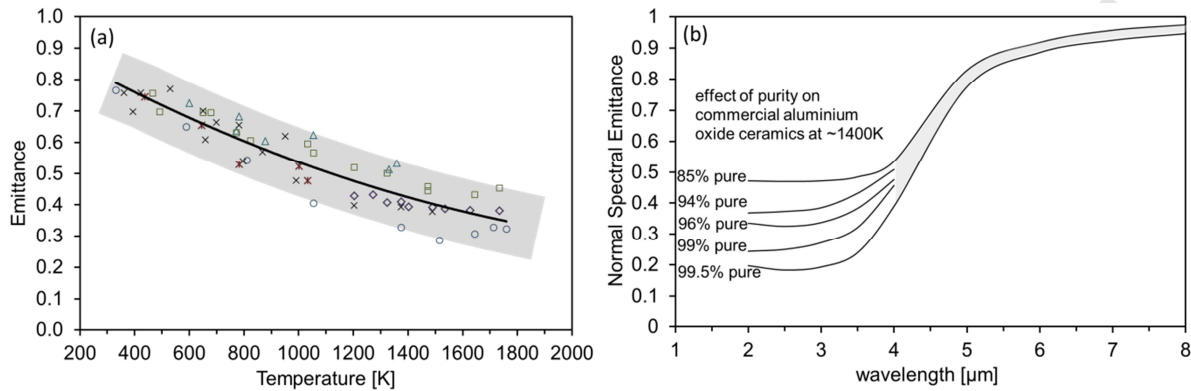


**Fig 2.** (a) Normal total emittance of aluminium oxide as a function of temperature showing experimental scatter, (b) the effect of purity on the normal spectral emittance of aluminium oxide at ~1400 K. Based on [8].

Tables A1 to A3 given in the Appendix list the total normal emissivity,  $\varepsilon_0(T)$  of a wide range of materials as a function of temperature (in Kelvin). These are expressed as least squares polynomials fitted to data from the references listed in the Tables by the expression:

$$\varepsilon_0(T) = a + 10^{-5}bT + 10^{-8}cT^2 + 10^{-10}dT^3 \quad (7)$$

where a, b, c, d are fitted coefficients. Omitted entries should be taken as zero. Extrapolation beyond the quoted temperature range should be undertaken with caution especially for strongly non-linear relationships where the c and d coefficients are non-zero.

Table A1 lists the emissivity of various pure metals, alloys and metals coated with oxides [7,23-32], and in this Table many of the constants for the polynomial equation have been taken from Reference [6].

**Figs 3 (a) and (b)** show plots for selected materials used in high temperature applications, typically in furnaces, or for temperature measurements. **Fig 3 (a)** shows some of these pure metals such as platinum and others which may become coated with the oxide films, namely, iron/steel [23-26], molybdenum [25], nickel [27], vanadium and tungsten [25] and titanium [28,29], as well as some alloys [30-32].

Because the oxide film is semi-transparent to radiation the spectral radiation properties of oxidized materials are related to the nature and thickness of the oxide film [32]. **Fig 3 (b)** gives information on solid  $\text{Fe}_2\text{O}_3$  which is markedly different to that as a film of oxide on metallic iron shown in **Fig 3 (a)**. Otsuka et al. [25] examined the emissivity of stainless steel and pure metallic molybdenum and tungsten and with protective layers. The emissivity measured at oxidation temperatures of 500–1000°C were higher than the data for polished metal given in the literature. Thus, metal oxides have higher hemispherical total emissivities than polished metals. Fu et al. [26] measured the total hemispherical emissivity of iron-based alloys as well as pre-oxidized samples at temperatures of 400°C and 600°C for several hours. Little happened at 400°C but the emissivities of samples oxidized at 600°C increased significantly with oxidation time. Iuchi et al. [32] developed a spectral emissivity model for metal oxide films, although its application is quite complex.

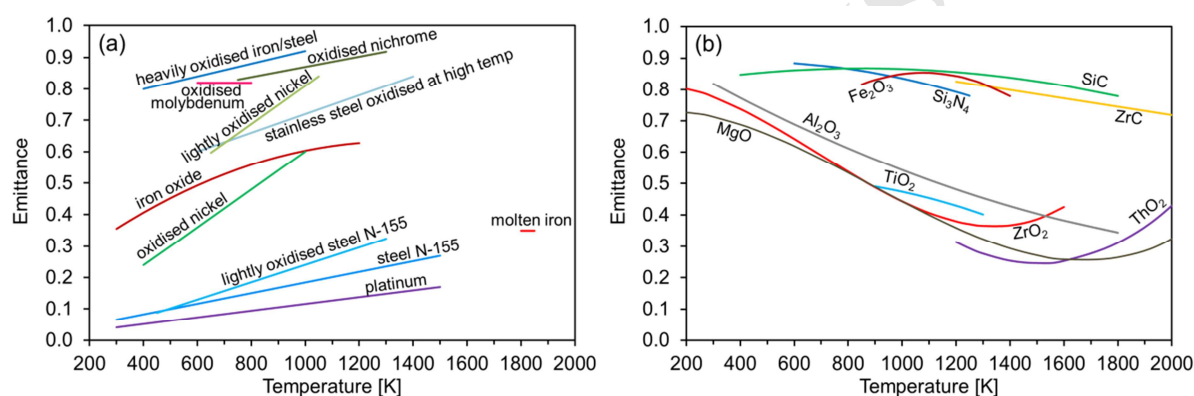


**Fig 3.** Total emittance of (a) some metals and (b) some inorganic oxide and refractories.

Data for refractory materials and glasses are given in Table A2 [33-46]; again many of the polynomial constants are taken from Reference [6]. **Fig 3 (b)** shows the complex variation with temperature for refractory materials. The ultra-high temperature ceramics, which are often darker and consist of conducting materials such as carbides, nitrides and borides, have high emissivities over the temperature range. The light coloured aluminium, magnesium and titanium oxides have a high emissivity at low temperatures but decreasing at furnace temperatures to about half their initial value. Zirconium and thorium oxides which become electrically conducting at higher temperatures show a minimum at furnace temperatures.

**Fig 4** shows data for a number of glasses and which exhibit only small experimental variation and are relatively well defined. The high silica containing glasses have the lower emissivities and the aluminium and boron containing glasses have the higher emissivities.

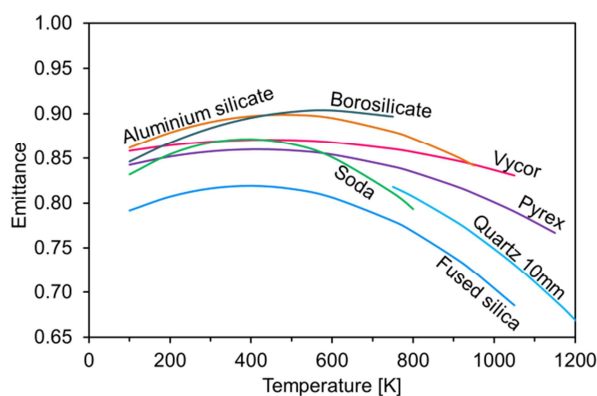


**Fig 4.** Normal total emittance of some glasses as a function of temperature.

The differences in the values of the emissivities obtained for a range of refractory furnace lining materials are highlighted in **Fig. 5**. This is because they are not only dependent on the material but also on their physical characteristics [33-44]. Their properties depend on whether they are covered in deposits such a slag in coal or oil fired furnaces, or sometimes in the case of oil flames with soot or carbon.

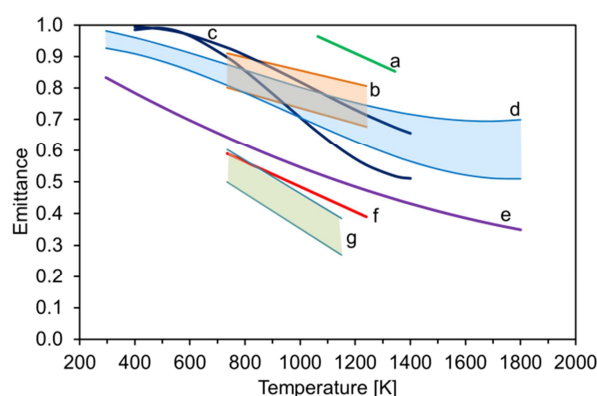


**Fig 5.** Normal total emittance of refractory materials based on aluminium and silicon oxides: (a) carborundum-based high emissivity coating [41]; (b) permeable ceramic materials [43]; (c) ceramic fibres (normal, [40] and parallel, [40]); (d) silica bricks [43]; (e)  $\text{Al}_2\text{O}_3$  mean line from Fig. 2; (f) ceramic fibre board (44); (g) light-weight refractory [41].

Table A3 lists data for surface coatings. These coatings usually consist of a thin layer of protective refractory against the surrounding atmosphere which is usually oxidative. Here there is some overlap with the data in Table A2 where high emissivity furnace coatings are listed. The purpose of these is to increase the emissivity and also to offer some surface protection, but usually the surface layer is not coherent and does not offer full oxidative protection. This topic is discussed more fully in Section 5.

Table A4 lists data for biomass, carbons, chars [46-60] and fuel ash deposits [62-67]. The combustion of coal, oil and more recently solid biomass, with air or oxygen in a refractory lined combustion chamber or boiler has attracted considerable research on their radiant properties in order to improve their efficiency or minimise pollution. Because the emissivity changes during the combustion process these are set out here. In a pulverised fuel combustor the combustion of solid fuel particles, whether coal or biomass, goes through the following steps: heating up of the fuel particle, devolatilisation, the formation of char followed by the burn-out of the char leaving an ash [52,53]. The fuel, which initially will have complex band spectra [54-56], rapidly undergoes devolatilisation within ~0.1s and forms a carbonaceous char containing ash; then the char then burns out over a period of several seconds at temperatures of about 1800 K finally leaving ash. Solomon et al. [54] investigated devolatilising coal and the char formed finding a value for char of 0.7 at 1000K and that for devolatilising coal less than that. Bhattacharya and Wall [56] found the emittance of coal particles increases, up to a value of about 0.83 at 1473K with increase in the extent of devolatilisation, incompletely devolatilised coal is non-grey, particularly up to 7  $\mu\text{m}$  wavelength.

This transition from a char particle to mainly an ash particle is complex since as the ash becomes the dominant species it may change phase. If the particle is above the ash fusion temperature it becomes a liquid droplet but still containing some unreacted carbon which burns out forming a cenosphere may in turn fragment. The behaviour can in principle be tracked in CFD models. The char will have the grey body spectral behaviour of a carbon. The ash, consisting mainly of an alumino-silicate material containing some calcium and/or iron, behaves like a refractory material following the typical behaviour of the compounds shown in Fig. 5. Their emissivity is a function of the composition, particularly the iron content [3,19,57]. The emissivity of these char/ash particles have been measured in flames as well as at lower temperatures by a number of groups [10,19,55,56, 58-60] and the results are summarised in Table A 4. The low emissivities at high temperature are confirmed by measurements directly in flames [60-62].

The emissivity of a burning coal or biomass char particle changes as it reacts to become an ash particle. The change can be approximated by combining the  $\epsilon$  values of, for example, biomass char and wood ash given in Table A4 as follows:

$$\epsilon = 0.85(\text{mass fraction of char}) + (0.95 - 3 \times 10^{-4}T)(\text{mass fraction of ash}) \quad (8)$$

where the emissivity of the char is assumed to be 0.85 and that of the ash taken to a temperature dependent value from Table A4. Similar expressions can be derived using  $\epsilon$  values for coal chars and ashes.

The temperature is all important here, because in most furnace applications, it determines the fuel burn-out and hence emissivity, and also the ash deposition on the walls. Molten ash deposition on the refractory walls or boiler tubes is important and data on the emissivity of slag covered walls is available and a summary is given in Table A4. The emissivity varies with the chemical composition of the slag and the iron and silica contents are important, as well as the physical nature of the surface, ie molten or sintered ash and on particle size [3,17,19,64] or whether a phase change takes place [18,66]. The influence of rough surfaces, whether due to dust layers or sintering, is discussed in Section 4. This information is of considerable importance for the design of furnaces [3,15,64,67]. A correlation linking the emissivity to the iron content has been derived [67] based on an earlier correlation by Konopeiko in 1972 (see reference [67]). The thermal radiation from the combustion chamber results from the complex interplay between the hot combustion gases, the furnace walls and any particulate matter arising from the combustion process [1-3].

The directional emissivity,  $\epsilon_\theta$ , of a diffuse surface is independent of direction and this is often a reasonable assumption for many real materials [1,5]. Nevertheless, all surfaces exhibit some departure from diffuse behaviour and the general trends for the two special kinds of material discussed already, non-conductors and conductors, may be summarised as follows. For conductors,  $\epsilon_\theta$  is approximately constant for  $\theta < 40^\circ$ , increases up to about  $80^\circ$  and drops to zero at  $90^\circ$ . For insulators,  $\epsilon_\theta$  is roughly constant for  $\theta < 70^\circ$  after which it drops sharply. The net result of these trends is that the hemispherical emissivity does not differ markedly from the normal emissivity [1], their ratio being 1.0 to 1.3 for conductors and 0.95 to 1.0 for insulators as shown in **Fig 6**.

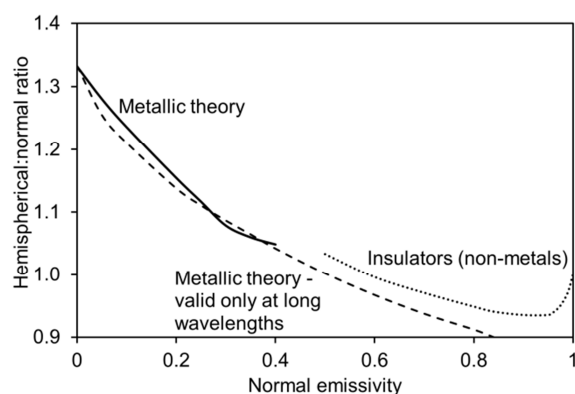


**Fig 6.** Ratio of hemispherical to normal emissivity as a function of normal emissivity for metals and non-metals. Based on [1].

From this data and associated literature it may be observed that:

1. The emissivity of clean metallic surfaces is small, being as low as 0.02 for polished gold and silver, although slowly increasing with temperature.
2. Oxidation of the metal surface markedly increases the emissivity, up to about 0.8 for heavily oxidised stainless steel for example.
3. The emissivity of conductors increases with increase in temperature, that of insulators will generally decrease. Some metal oxides become semi-conductors at high temperatures, and these exhibit a U shaped emissivity curve.
4. The total emissivity of ceramics at high temperatures is generally around 0.6 but there is some variation in the values depending on the composition.
5. The spectral emittance of most refractory materials is quite low (typically less than 0.6) at wavelengths less than 5-6 $\mu$ m so that at higher temperatures over around 1000K, the total emissivity tend to be lower at around 0.4 to 0.3.
6. There is a correlation between the variation of emissivity with temperature and wavelength because increasing the temperature of emission is accompanied by a decrease in the wavelength of that radiation.

#### 4. EMISSIVITIES OF ROUGH SURFACES SUCH AS REFRACTORIES

The surface roughness ( $r'$ ) can be expressed as the ratio of the root mean square depth of the cavities ( $d$ ) to the wavelength of radiation ( $r' = d/\lambda$ ) [1]. Surface roughness can be placed in two categories according to this criterion, bearing in mind that at very small values of  $r'$  the surface will be a smooth specular reflector.

- With relatively small cavities, the specular reflecting material is converted to a partially diffuse, partially specular reflector.
- Multiple reflections occur with surfaces possessing relatively deep cavities and the effective emissivity is significantly larger than that of a smooth surface.

The first category has been treated by Porteus and Porteus [69], among others. A simple approach to the second category is given by examining a single cavity as shown in **Fig. 7**. An imaginary plane of area  $A_2$  is stretched across a cavity of area  $A_1$ . The analysis [55] of radiative flux leaving  $A_1$  shows that the cavity can be replaced by the plane area  $A_2$  with effective emissivity given by Eq.9.

$$\varepsilon_2 = \varepsilon_1 / (1 - \rho_1(1 - A_2/A_1)) \quad (9)$$

where  $\rho$  and  $\varepsilon$  refer to reflectivity and emissivity. For a groove of angle  $60^\circ$ , for example, the emissivity is increased by varying amounts, depending on the original emissivity, as shown in Table 1. Consequently, the apparent emissivity of a diffuse furnace wall can be enhanced by cutting grooves in the surface.

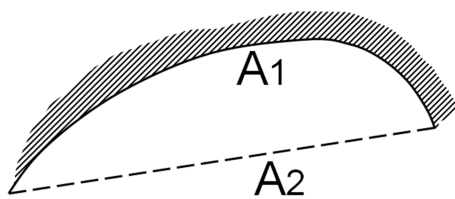


**Fig 7.** Representation of a cavity by an imaginary plane surface.



**Table 1.** The effect of surface roughness on enhancing emissivity (groove angle 60°).

Actual Emissivity	Enhanced Apparent Emissivity
0.1	0.18
0.2	0.33
0.3	0.46
0.4	0.57
0.5	0.67
0.6	0.75
0.7	0.82
0.8	0.89

Certain materials which are granular or fibrous are inherently rough. The radiative properties of granular metal oxide refractories and fibrous materials are determined not by the surface layer but by scattering and adsorption by particles below the surface. The calculation of values of emissivity has been made but it is not easy to predict values accurately for real materials. The effect of grain size and material has been indicated by experimental measurements at 1200°C as shown in Table 2 [1]. A typical granular refractory brick with a grain size of 60 µm would have grooves in the surface with an angle of approximately 60° and an enhancement of emissivity as given by the values in Table 1. A ceramic fibre board would also contain grooves of about 60°, whilst some stack-bonded boards would have a greater increase. Rough surfaces should lead to higher emissivities for a particular material. This is particularly true for metals [71]. There is some evidence, from **Fig.5**, that it is also true when comparing certain refractory materials, but it is difficult to isolate this effect from differences in composition between these materials, even when these are small since minor variations in the amounts of certain compounds can affect emissivity (cf Table A2). However, for the same material composition, it has proved difficult to measure the effects of varying surface emissivity since, by nature, refractory materials are diffuse emitters and reflectors [1,41] and this aspect is not very affected by surface roughness in comparison to metals where the differences in surface behaviour can be greater between polished and oxidised surfaces.



**Table 2.** Effect of Grain Size on the Emissivity of Selected Oxides measured at 1200°C, taken from [1].

Oxide	Grain size ( $\mu\text{m}$ )	Emissivity
$\text{Al}_2\text{O}_3$	2 - 25	0.35
	15 - 80	0.43
	90 - 120	0.53
$\text{MgO}$	1 - 3	0.30
	30 - 75	0.39
	90 - 120	0.48
$\text{Cr}_2\text{O}_3$	0.5 - 1.5	0.72
	1.5 - 8	0.95

## 5. SURFACE COATINGS

The theory of optical surface coatings is well developed for optical components and for solar radiation applications where surfaces are of a regular shape [5]. In the case of non-uniform surfaces such as furnace insulation materials the surface is less well defined. There are a number of applications where surfaces are deliberately coated to increase surface emissivity or for surface protection [1,5]. An important class of the application of surface coatings are those used to enhance surface emissivity in industrial furnaces, and some examples are given in Table A3 and in Fig. 5. Generally, those coatings contain iron or silicon carbide to enhance the emissivity and the effects are shown in the Table. It is not surprising that these coatings also tend to be darker in appearance. However, these coatings are only advantageous in certain furnace applications where the stock is only heated intermittently, for instance in some continuous heating processes, rather than where there is steady state heating, in which case the furnace wall emissivity is immaterial since the furnace behaves as a black body enclosure [41,42, 68].

An important example of protection is the use of silica films to prevent catalytic reactions of platinum-based thermocouples in flames. The results of such computations for coated wire temperatures of 577, 977 and 1450°C are shown in **Fig. 8**, where data for the total hemispherical emittance is given against the overall diameter of the coated wire [72].

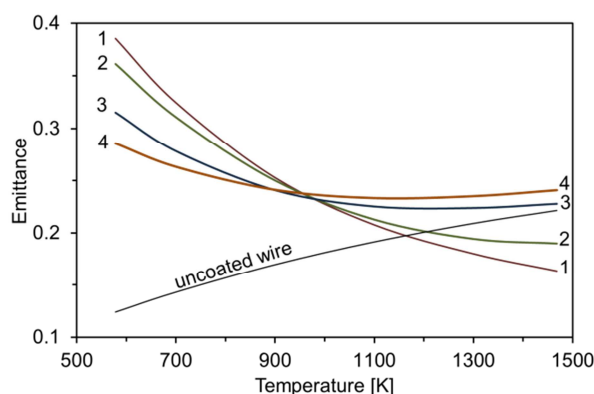


**Fig 8.** Variation of total hemispherical emittance with temperature for different thicknesses of coating on a thermocouple. Assumed thermocouple diameter 12.7  $\mu\text{m}$ ; coatings (1) 53.3  $\mu\text{m}$ ; (2) 38.1  $\mu\text{m}$ ; (3) 22.9  $\mu\text{m}$ ; (4) 17.8  $\mu\text{m}$ . Based on [72].

At the lowest temperature there is a continuing rise of emissivity with coating thickness and this is because an appreciable proportion of the radiant energy originates in the silica coating. At temperatures of 977 and 1450°C a different effect is observed. A very thin coating gives rise to an increase in emissivity owing to emission from the silica. A further increase in thickness eventually leads to a decreasing emittance owing to the decreasing amount of radiation from the unit area of the outside surface which has originated at the core. This decrease is not compensated by an increased emission from the silica for at higher temperatures black-body emission resides increasingly in the lower wavelength region where the silica is almost transparent. **Fig. 8** shows the variation of emissivity with temperature for the different thicknesses of coating. At the lower temperatures the coating produces a marked increase in emittance, but as the temperature increases this effect is reduced.

## CONCLUSIONS

The effect of temperature on the emissivity of various materials used in high temperature applications has been compiled. The data shows that the total normal emissivities of the more commonly used materials in furnace construction are typically in the range 0.4 to 0.8. However there can be considerable uncertainty particularly in materials used in engineering applications due to a lack of knowledge of the accurate surface temperature, and the exact physical or chemical surface properties.

A considerable body of information is available relating to the combustion of coal and biomass fuels especially particulate fuels. The behaviour of particulate char is complex as it burns out to form an ash which may then be deposited on the furnace walls, but the process can be tracked.

## ACKNOWLEDGEMENTS

The authors are grateful to Dr Edward Hampartoumian, Mr Douglas Hainsworth and Mr John M. Taylor for their work for the original version of this paper. We thank Dr Albino Reis for help in accessing information. We are also grateful to the Reviewers for their helpful comments.

## REFERENCES

- [1]. H.C. Hottel, and A.E. Sarofim, Radiative heat transfer, McGraw Hill, New York, 1967.
- [2]. R. Viskanta, M.P. Mengoc, Radiation heat transfer in combustion systems, Prog. Energy Combust. Sci. 13 (1987) 97-160.
- [3]. T.F. Wall, A. Lowe, L.J. Wibberly, I. McC. Stewart, Mineral matter in coal and the thermal performance of large boilers, Prog. Energy Cornbust. Sci. 5, (1979) 1-29.
- [4]. F P Incropera, D.P. DeWitt, T.L. Bergman, A.S. Lavine, Introduction to Heat Transfer. John Wiley 2007 6th edition
- [5]. M.F. Modest, Radiative Heat Transfer, 3rd Edition 2013 Elsevier Oxford
- [6]. E. Hampartsoumian, D. Hainsworth, J.M. Taylor, A. Williams, The radiant emissivity of some materials at high temperatures-review, J. Inst. Energy 74 (2001) 91-99.
- [7]. Y.S. Touloukian, D.P. DeWitt, Thermal radiative properties: Metallic elements and alloys, 1970, Vol. 7; in Thermophysical Properties of Matter, TPRC Data Series (edited by Y.S Touloukian, C.Y. Ho) IFI/Plenum Press, New York.
- [8]. Y.S Touloukian, D.P. DeWitt, Thermal radiative properties. Non-metallic solids, 1971, Vol. 8; in Thermophysical Properties of Matter, TPRC Data Series (edited by Y.S. Touloukian, C.Y. Ho) IFI/Plenum Press, New York.
- [9]. D.G.Elliston, W.A. Gray, D.F. Hibberd, T-Y Ho, A. Williams, The effect of surface emissivity on furnace performance, J. Inst. Energy (1987) 155-167.
- [10]. S. Rego-Barcena, R. Saari, R. Mani, S. El-Batroukh, M.J. Thomson, Real time, non-intrusive measurement of particle emissivity and gas temperature in coal-fired power plants, Meas. Sci. Technol. 18 (2007) 3479–3488.
- [11]. L. Ma, M. Gharebaghi, R. Porter, M. Pourkashanian, J.M. Jones, A. Williams. Modelling methods for co-fired fuel furnaces, Fuel, 88, 2448-2454, 2009.

- [12]. G. Krishnamoorthy, C. Wolf, Assessing the role of particles in radiative heat transfer during oxy-combustion of coal and biomass blends, *J. Combust*, (2015) Article ID 793683.
- [13]. Fluke Process Industries, [www.flukeprocessinstruments.com/en-us/about-us/infrared-technology](http://www.flukeprocessinstruments.com/en-us/about-us/infrared-technology)
- [14]. A.M. Vassallo, P.A. Cole-Clarke, L. S. K. Pang, A.J. Palmisano, Infrared emission spectroscopy of coal minerals and their thermal transformations, *Appl Spectrosc.*, 1992, 46 (1) 73-78.
- [15]. C.J. Zygarlicke, D.P. McCollor, C.R. Crocker, Task 3.2 – Ash Emissivity Characterization and Prediction, December 1999. U.S. Department of Energy – NETL; Report No. 99-EERC-12-05.
- [16]. S. Bohnes, V. Scherer, S. Linka, M. Neuroth, H. Bruggemann, Spectral emissivity measurements of single mineral phases and ash deposits, *Proc. 2005 Summer Heat Transfer Conference*, July 17-22 San Francisco, Calif, USA HT2005-72099. pp 175–182.
- [17]. F. Greffrath, J. Gorewoda, M. Schiemann, V. Scherer, Influence of chemical composition and physical structure on normal radiant emittance characteristics of ash deposits, *Fuel* 134 (2014) 307–314.
- [18]. J. Gorewoda, V. Scherer, Normal radiative emittance of coal ash sulfates in the context of oxyfuel combustion, *Energy Fuels* 31 (2017) 4400–4406.
- [19]. T.F. Wall, H.B. Becker, Total absorptivities and emissivities of particulate coal ash from spectral band emissivity measurements, *J Eng Gas Turbines Power*, 106 (1984) 771-776.
- [20]. T.F. Wall, S.P. Bhattacharya, D.K.Zhang, R.P. Gupta, X. He, The properties and thermal effects of ash deposits in coal-fired furnaces, *Prog. Energy Combust. Sci.* 19 (1993) 487-504.
- [21]. *Handbook of Chemistry and Physics* (60th Edition), CRC Press, Boca Raton, Florida, 1981.
- [22]. M. Shimogori, F. Greffrath, V. Scherer, A. Gwosdz, C. Bergins, Spectral emissivities of Ni and Fe based boiler tube materials with varying chromium content at high temperature atmospheres, 27th Annual International Pittsburgh Coal Conference 2010, Istanbul, Turkey, October 2010, 1940-1954.
- [23]. P. Ratanapuech, R.G. Bautista, Normal spectral emissivities of liquid iron, liquid nickel and liquid iron-nickel alloys, *High Temp. Sci.*, 1981, 14(4) 269-283.
- [24]. M. Susa, R.K. Endo, Emissivities of High Temperature Metallic Melts, *Advances in Materials Research Book Series* ( volume 11)

- [25]. A. Otsuka, K. Hosono, R. Tanaka, K. Kitagawa, N. Arai, A survey of hemispherical total emissivity of the refractory metals in practical use, *Energy* 30 (2005)
- [26]. T. Fu, P. Tan, M. Zhong, Experimental research on the influence of surface conditions on the total hemispherical emissivity of iron-based alloys, *Exp. Therm. Fluid Sci.*, 40 (2012) 159–167
- [27]. T.R. Fu, P. Tan, J. Ren, H.S. Wang, Total hemispherical radiation properties of oxidised nickel at high temperatures, *Corros. Sci.* 83 (2014) 272-280.
- [28]. G. Teodorescu Radiative Emissivity of Metals and Oxidised Metals at High Temperature, PhD Thesis Auburn University, 2007
- [29]. G. Teodorescu, P.D. Jones, R.A. Overfelt, B. Guo, High temperature emissivity of high purity titanium and zirconium. 16th Symposium on Thermophysical Properties Boulder (2006)
- [30]. B.P. Keller, S.E. Nelson, K.L. Walton, T. K. Ghosh, R.V. Tompson, S. K. Loyalka, Total hemispherical emissivity of Inconel 718, *Nuc. Eng. Des.* 287 (2015) 11–18
- [31]. P. Hagqvist, F. Sikström, Anna-Karin Christiansson, Emissivity estimation for high temperature radiation pyrometry on Ti–6Al–4V, *Measurement* 46 (2013) 871–880.
- [32]. T. Iuchi, T. Furukawa, S. Wada, Emissivity modeling of metals during the growth of oxide film and comparison of the model with experimental results, *Appl. Opt.* 42 (2003) 2317–2326.
- [33]. P.D. Osborn, *Handbook of Energy Data and Calculations*. Butterworth, London, 1985.
- [34]. J.D. Jackson, E. Romero, J.J. Norris, Comparison of Techniques for the measurement of the emittance of ceramic materials. *Ceramics in Energy Application*, The Institute of Energy, London (1994) 133-148.
- [35]. V.A. Petrov, V.Yu Reznik, Measurement of the emissivity of quartz glass, *High Temp-High Press* 4 (1972) 687-693.
- [36]. J.A. Wieringa, J.J.Ph. Elich, C.J. Hoogendoorn, The spectral emissivity of glass furnace roofs and the effect on heat transfer, *Ceramics in Energy Applications Conference*, Sheffield, IOP Publishing Ltd. (1990) 159-168.
- [37]. A. Williams, E. Hampartsoumian, B. Simmons. Unpublished data, 1988.
- [38]. L. Mercatelli, E. Sani, D. Jafrancesco, P. Sansoni, D. Fontani, M. Meucci, S. Coraggia, L. Marconi, J.-L. Sans, E. Beche, L. Silvestroni D. Sciti, Ultra-refractory diboride ceramics for solar plant receivers, *Energy Procedia* 49 ( 2014 ) 468 – 477.

- [39]. Zhang, J. Dai, X. Lu, Y. Wu, Effects of temperature on the spectral emissivity of C/SiC composites, *Ceramics-Silikáty* 60 (2) (2016) 152-155.
- [40]. J.D. Fletcher, A. Williams, Emissivities of ceramic fibre linings for high-temperature furnaces. *J. Inst. Energy* (1984) 377.
- [41]. E. Hampartsoumian, Spectral emittance measurements of furnace wall materials and coatings. *Ceramics in Energy Applications Conference*, Sheffield, IOP Publishing Ltd, (1990) 149-157.
- [42]. I. Alexander, W.A. Gray, E. Hampartsoumian, J.M. Taylor, Surface emissivities of furnace linings and their effect on heat transfer in an enclosure, *1st European Conference on Industrial Furnaces and Boilers*, (1988) Lisbon, 59-68.
- [43]. J.D. Jackson, C-C Yen, Measurements of total and spectral emissivities of some ceramic fibre insulation materials. *Ceramics in Energy Applications*, The Institute of Energy, London, 1994, 159.
- [44]. J.D. Jackson, P. An, I. Pena-Marco, Measurements of the total and spectral emittance of permeable ceramic materials. *Proc. 4<sup>th</sup> UK National Heat Transfer Conference*, C510/132, *I. Mech. E.* (1995) 561-565.
- [45]. J.A. Wieringa, Spectral radiative heat transfer in gas-fired furnaces. PhD Dissertation, *Technische Universiteit Delft*, (1992).
- [46]. G. Fisher, Ceramic coatings enhance performance engineering, *Ceramic Bull.*, 65 (1986) 283-287.
- [47]. G. Neuer, G. Jaroma-Weiland, Spectral and total emissivity of high temperature materials, *Int. J. Thermophys.* 19 (1998) 917-929.
- [48]. G. Lopez, L.A. Bastera, L. Acuna, M. Casado, Determination of the emissivity of wood for inspection by infra-red, *J. Nondestruct. Eval.* 32 (2013) 172-176.
- [49]. T. Matsumoto, T. Koizumi, Y. Kawakami, K. Okamoto, M. Tomita, Perfect blackbody radiation from a graphene nanostructure with application to high temperature spectral emissivity measurements, *Opt. Express* 21 (2013) 30964-30974.
- [50]. D.D. Evans, H.W. Emmons, Combustion of wood charcoal, *Fire Research* 1 (1977) 57-66.
- [51]. J. Saliero, A. Gomez-Barea, M. Tripiana, B. Leckner, Measurement of char surface temperature in a fluidized bed combustor using pyrometry with digital camera, *Chem. Eng J.* 288 (2016) 441-450.

- [52]. R.I. Backreedy, L.M. Fletcher, L. Ma, M. Pourkashanian, A. Williams, Modelling pulverised coal combustion using a detailed coal combustion model, *Combust. Sci. Technol.* 178 (2006) 763-787.
- [53]. L. Ma, J.M. Jones, M. Pourkashanian, A. Williams, Modelling the combustion of pulverised biomass in an industrial furnace, *Fuel*, 86, (12, 13) (2007) 1959-1965.
- [54]. P.R. Solomon, R.M. Carangelo, P.E. Best, J.R. Markham, D.G. Hamblen, The spectral emittance of pulverized coal and char, *Proc. Combust. Symp.* 21 (1986) 437-446.
- [55]. L.L. Baxter, T.H. Fletcher, D.K. Ottesen, Spectral emittance measurements of coal particles, *Energy Fuels* 2 (1988) 423-30.
- [56]. S.P. Bhattacharya, T.F. Wall, Development of emittance of coal particles during devolatilisation and burnoff, *Fuel* 78 (1999) 511-519.
- [57]. J. Boow, P.R.C. Goard, Fireside deposits and their effect on heat transfer in a pulverized-fuel-fired boiler: Part III. The Influence of the physical characteristics of the deposit on its radiant emittance and effective thermal conductance. *J Inst Fuel* 42 (1969) 412-419.
- [58]. P.R. Solomon, R.M. Carangelo, P.E. Best, J.R. Markham, D.G. Hamblen, The spectral emittance of pulverized coal and char, *Proc. Combust. Inst.* 21 (1986) 437-446.
- [59]. P. Graeser, M. Schiemann Char particle emissivity of two coal chars in oxy-fuel atmospheres, *Fuel* 183 (2016) 405-413.
- [60]. P. Graeser, M. Schiemann Emissivity of burning bituminous coal char particles-burnout effects *Fuel* 196 (2017) 336-343.
- [61]. D. Backstrom, R. Johansson, K.J. Andersson, F. Johnsson, S. Clausen, A. Fateev, Measurement and Modeling of particle radiation in coal flames, *Energy Fuels*, 28(3) (2014) 2199-2210.
- [62]. S. Yipeng, L. Chun, Z. Huaichun, A simple judgment method of gray property of flames based on spectral analysis and the two-color method for measurements of temperatures and emissivity, *Proc. Combust. Inst.* 33 (2011) 735-741.
- [63]. J.R. Markham, P.E. Best, P.R. Solomon, Z.Z. Yu. Measurement of radiative properties of ash and Slag by FT-IR emission and reflection spectroscopy. *Trans. ASME* 114 (1992) 458-464
- [64]. A. Zbogor, F.J. Frandsen, P.A. Jensen, P. Glarborg, Heat transfer in ash deposits: A modelling tool-box. *Prog Energy Combust Sci.* 31 (2005) 371-421.
- [65]. F. Greffrath, J. Gorewoda, M. Schiemann, V. Scherer, Influence of chemical composition and physical structure on normal radiant emittance characteristics of ash deposits. *Fuel* 2014;134:307-14.



- [66]. J. Gorewoda, V. Scherer, Influence of carbonate decomposition on normal spectral radiative emittance in the context of oxyfuel combustion, *Energy Fuels* 30 (2016) 9752–9760.
- [67]. M. Shimogori, H. Yoshizako, Y. Matsumura, Determination of coal ash emissivity using simplified equation for thermal design of coal-fired boilers, *Fuel* 95 (2012) 241–246.
- [68]. Y.U. Khan, D.A. Lawson, R.J. Tucker, Analysis of radiative heat transfer in ceramic-lined and ceramic-coated furnaces, *J. Inst. Energy* 71 (1998) 21–27.
- [69]. H.E Bennet, J.D. Porteus, Relation between surface roughness and specular reflectance at normal incidence, *J. Opt. Soc. Am.* 51 (1961) 123–129.
- [70]. W.A. Gray, R. Müller, *Engineering Calculations in Radiant Heat Transfer*, Pergamon Press, Oxford, 1974.
- [71]. D.P. De Witt, R.S. Bernicz, *Temperature, Its Measurement and Control in Science and Industry*, 4, 1 Reinhold Publishing, 1972.
- [72]. D Bradley, A.G. Entwistle, The total hemispherical emittance of coated wires, *Brit. J. Appl. Phys.* 17 (1966) 1155–1164.



## 546 APPENDIX

547 TABLE A1

Metals		a	b	c	temp range K	ref	$\epsilon$ range
Aluminium	polished	0.0263	5.01		300 - 900	7	0.04-0.07
	oxidised	0.0463	5.01		450 - 900	7	0.07-0.09
	lightly oxidised	0.011	21		473 - 873	7	0.11-0.19
Brass	polished	0.03			550	1	0.03
	unoxidised	0.035			295	1	0.04
	oxidised @ 599°C	0.6			573 - 873	1	0.6
Copper	polished	0.021	1.98		300 - 1200	7	0.03-0.05
	oxidised, red heat 30 min	0.06	15.4		400 - 1050	7	0.12-0.22
	oxidised at 1000 K		80		600 - 1000	7	0.48-0.8
	thick oxide	0.72	20		400 - 1000	7	0.8-0.92
Gold		0.0432	-8.88	7.15	600 - 1000	7	0.02-0.026
Iron/steel	polished		18.2		100 - 1050	7	0.24-0.61
	iron oxide, red heat 30 min	0.173	68.6	-25.6	100 - 1050	7	0.24-0.61
	molten	0.35			1810 - 1860	23	0.35
	heavily oxidised	0.72	20		400 - 1000	7	0.8-0.92
Stainless steels	N-155, oxidation retarded	0.0144	17		100 - 1500	7	0.031-0.27
	N-155, lightly oxidised	-0.0372	27.8		450 - 1300	7	0.09-0.32
	oxidised at high temp.	0.42	30		600 - 1400	7	0.60-0.84
	heavily oxidised	0.72	20		400 - 1000	7	0.8-0.92
Molybdenum	polished	0.0288	12.7		100 - 1800	7	0.04-0.26
	oxidised	0.82			600 - 800	7	0.82
Nickel	polished	0.014	12.9		100 - 1500	7	0.03-0.21
	oxidised		60		400 - 1000	7	0.24-0.6
	unoxidised	0.01	13.3		723-1123	27	0.1-0.16
	Ni oxidised to various degrees {	0.266	24		723-1123	27	0.43-0.5
		0.4	17.8		723-1123	27	0.5-0.6
Nichrome	clean	0.65			323	21	0.65
	oxidised	0.71	16		773 - 1273	21	0.83-0.91
Palladium	polished	-0.03	11.7		400 - 1550	7	0.03-0.16
Platinum	polished	0.008	10.8		100 - 1500	7	0.02-0.17
Silver	electrolytic	0.0119	1.9		400 - 1200	7	0.02-0.035
Titanium		0.913	-96.9	36.5	1373-1673	28,29	0.27-0.31
	lightly oxidised	0.2	61		673 - 1023	7	0.6-0.82
Tin	polished	0.0085	10.8		300 - 500	7	0.041-0.06
Tungsten	polished	-0.003	10.5		273-2500	7	0.03-0.26
Zinc	polished	-0.01	10		500 - 600	1	0.04-0.05
	oxidised at 400°C	0.11			673	1	0.11
Inconel-718		0.11	13.2		760-1275	30	0.21-0.28
Ti-6Al-4V		0.165	31.5	-15.5	773-1323	31	0.3-0.33

548

549 TABLE A2

Non-metals		a	b	c	d	temp range K	ref	$\epsilon$ range
Alumina		0.98	-53	10.2		300 - 1800	8	0.83-0.35
Fire brick (Al/Si/Fe/O)	low Al <sub>2</sub> O <sub>3</sub> content	0.9	-10			673 - 1673	33	0.83-0.73
	medium Al <sub>2</sub> O <sub>3</sub> content	0.84	-20			673 - 1673	33	0.71-0.51
	high Al <sub>2</sub> O <sub>3</sub> content	0.8	-20			673 - 1673	33	0.64-0.39
Fired-Clay:	63.2% Al <sub>2</sub> O <sub>3</sub> , 32.1 SiO <sub>2</sub>	0.74	133	-268	11.8	300 - 1300	34	0.90-0.55
Glasses	Vycor (Corning 7900)	0.85	9.5	-10.8		70 - 1050	8	0.87-0.85
	Aluminium silicate	0.84	24.6	-25.7		70 - 950	8	0.89-0.83
	Pyrex (Corning 7740)	0.83	14.4	-17.3		70 - 1150	8	0.86-0.8
	Borosilicate	0.82	28.7	-24.6		70 - 750	8	0.88-0.86
	Soda	0.8	36.6	-46.8		70 - 800	8	0.86-0.68
	Fused silica	0.77	24.8	-31.3		70 - 1050	8	0.75-0.71
	Quartz, 2 mm thick	0.61	25.8	-31.4		750 - 1200	35	0.65-0.41
	Quartz 10 mm thick	0.82	20.7	-27.6		750 - 1200	35	0.84-0.62
	Molten glass	0.8				1773	36	0.8
Iron oxide	(Fe <sub>2</sub> O <sub>3</sub> )	-0.01	161	-75		850 - 1300	8	0.75-0.85
Magnesium oxide	(MgO)	0.73	11.8	-65	2.48	500 - 2350	8	0.73-0.3
Silicon carbide	(SiC)	0.8	15.4	-9.01		400 - 1850	8	0.85-0.78
	polished	0.99				298 - 373	37	0.99
	oxidised (1h, 1367 K)	0.7	-25			800 - 1600		0.5-0.3
Silicon nitride	(Si <sub>3</sub> N <sub>4</sub> )	0.86	13.9	-16.3		600 - 1250	8	0.89-0.78
	polished	0.98				298 - 373	37	0.98
Thorium dioxide	(ThO <sub>2</sub> )	1.93	-224.1	74.7		1200 - 2250	8	0.32-0.67
Titanium dioxide	(TiO <sub>2</sub> )	0.68	-21.2			850 - 1300	8	0.49-0.4
	polished	0.95				298 - 373	37	0.96-0.95
Zirconia	(ZrO <sub>2</sub> )	0.82	6.67	-86.8	4.18	50 - 1600	8	0.82-0.42
Zirconia/MgO (1:1)		0.9	-37			700 - 1700	3	0.64-0.27
	polished	0.94				293 - 373	37	0.95-0.92
Zirconium carbide		0.98	-13.9			1200 - 2400	8	0.82-0.66
Zirconium dibromide	(ZrB <sub>2</sub> )	0.14	19			1100-1625	38	0.35-0.45
Hafnium dibromide	(HfB <sub>2</sub> )	0.14	19			1100-1625	38	0.35-0.45
TaB67-ceramics		0.54	10			1100-1625	38	0.65-0.7
C/SiC composites		0.727	15.5	-8.55		1000-2000	39	0.8-0.7
Ceramic fibre Board 45wt% Al <sub>2</sub> O <sub>3</sub> , 55wt% SiO <sub>2</sub> , 0.05wt% Fe <sub>2</sub> O <sub>3</sub>	fibres normal to surface	1.27	-48.5	2.84		600 - 1400	40	0.94 - 0.65
	parallel bonded fibres	1.47	-91.1	14.4		600 - 1400	40	0.9-0.48
Zirconia coated fibre		1.26	-26.7			1000 - 1300	9	0.99-0.91
Ceramic Fibres								
Kaowool	45wt% Al <sub>2</sub> O <sub>3</sub> , 55wt% SiO <sub>2</sub>	2.39	-165			923 - 1173	41	0.87-0.40
Zicar	99wt% ZrO <sub>2</sub>	0.51				1080	41	0.51
Saffil	95wt% Al <sub>2</sub> O <sub>3</sub> , 5wt% SiO <sub>2</sub>	0.49				1010	41	0.49
Microtherm	65wt% SiO <sub>2</sub> , 3.2wt% TiO <sub>2</sub>	0.48				950	41	0.48

550

551 TABLE A2 (continued)

Refractories		a	b	temp range K	ref	$\epsilon$ range
<b>Lightweight Refractories</b>						
PK 110	20wt% Al <sub>2</sub> O <sub>3</sub> , 53wt% SiO <sub>2</sub> , 4wt% Fe <sub>2</sub> O <sub>3</sub> , 16wt% MgO	0.43	14.4	1073-1350	41	0.58-0.62
MPK 125	36wt% Al <sub>2</sub> O <sub>3</sub> , 46wt% SiO <sub>2</sub> , 15wt% CaO	0.53	8	1063-1350	41	0.54-0.64
MPK 140	41wt% Al <sub>2</sub> O <sub>3</sub> , 54wt% SiO <sub>2</sub>	0.21	25.3	1073-1350	41	0.48-0.55
MPK 155HA	61wt% Al <sub>2</sub> O <sub>3</sub> , 36wt% SiO <sub>2</sub>	0.75	-27.9	1063-1350	41	0.44-0.36
MPK 130HSR	36wt% Al <sub>2</sub> O <sub>3</sub> , 54wt% SiO <sub>2</sub>	0.61		1073-1250	41	0.60-0.62
MPK SUPRA	11wt% Al <sub>2</sub> O <sub>3</sub> , 75wt% SiO <sub>2</sub> , 6wt% Fe <sub>2</sub> O <sub>3</sub>	-0.16	74	1073-1300	41	0.64-0.81
<b>Refractory Brick</b>						
alumina/silica : 330 kg/m <sup>3</sup> .	45wt% Al <sub>2</sub> O <sub>3</sub> , 55% SiO <sub>2</sub>				33	} see Fig 5
alumina/silica : 260 kg/m <sup>3</sup> .	45wt% Al <sub>2</sub> O <sub>3</sub> , 55% SiO <sub>2</sub>				33	
alumina/silica : 240 kg/m <sup>3</sup> .	50wt% Al <sub>2</sub> O <sub>3</sub> , 50% SiO <sub>2</sub>				33	
alumina/silica : 210 kg/m <sup>3</sup> .	50wt% Al <sub>2</sub> O <sub>3</sub> , 50% SiO <sub>2</sub>				33	
alumina/silica : 200 kg/m <sup>3</sup> .	70wt% Al <sub>2</sub> O <sub>3</sub> , 26% SiO <sub>2</sub>				33	
alumina/silica : 130 kg/m <sup>3</sup> .	45wt% Al <sub>2</sub> O <sub>3</sub> , 53% SiO <sub>2</sub>				33	
alumina/silica : 100 kg/m <sup>3</sup> .	45wt% Al <sub>2</sub> O <sub>3</sub> , 55% SiO <sub>2</sub>				33	
alumina/silica : 100 kg/m <sup>3</sup> .	100% SiO <sub>2</sub>				33	
alumina/silica : 80 kg/m <sup>3</sup> .	100% SiO <sub>2</sub>				33	
silica brick	97wt% SiO <sub>2</sub> , 2.6wt% CaO				35	
silica brick, used (as above)	97wt% SiO <sub>2</sub> , 2.6wt% CaO				35	
Zirconia silicate	32wt% SiO <sub>2</sub> , 63wt% ZrO				35	
<b>Furnace Refractory porous</b>						
80-90% Al <sub>2</sub> O <sub>3</sub> , 5-9%, SiO <sub>2</sub>	1.2 pores/mm	1.17	-50.6	750-1050	44	0.8-0.65
	0.8 pores/mm	1.13	-37.6	650-1050	44	0.88-0.74
	0.4 pores/mm	1.09	-29.8	850-1650	44	0.6-0.82

552

553 TABLE A3

Coatings	a	b	c	temp range K	ref	$\epsilon$ range
High Emissivity Furnace Coatings						
Carbide coating (bonded to refractory bricks)	0.97			273 - 1273	46	0.99-0.95
CaO stabilised Zr/Fe/Cr oxides	0.98			1273	46	0.98
Zirconia, unstabilised	0.98			813 - 1373	46	0.98
Carbonundum powder-based	1.56	-60		1023 - 1273	41	0.95-0.8
SiO <sub>2</sub> based	0.83			950 - 1373	41	0.84-0.81
ZrO <sub>2</sub> based	0.6			1073 - 1350	41	0.55-0.64
Furnace Wall Protective Coating						
NOVIT 62wt% ZrO <sub>2</sub> , 32wt% SiO <sub>2</sub>	1	-40		1073 - 1373	41	0.56-0.44
X-ray anode coatings						
STZ	1.06	260	87.9		47	0.66-0.86
Oxidation Protective Coatings for Reusable Space Vehicles						
Polysilazine (Si-C-N) + Si	0.82			1100-1700	47	0.82
Polysilazine (Si-C-N) + SiC	0.75			1100-1700	47	0.75

554

555 TABLE A4

Solid fuels		a	b	temp range K	ref	$\epsilon$ range
<b>Carbon</b>	Carbon, rough	0.81		300 - 2100	8	0.81
	Graphite, polished	0.81	2.2	0 3000	8	0.81-0.88
	Graphene			Up to 2500	49	0.99
	Candle soot	0.95		373-500	1	0.95
	Lampblack	0.96		323 - 1273	1	0.96
<b>Biomass Particles</b>						
Wood		0.9		295-337	48	0.92-0.86
Biomass charcoal	(large surface)	0.85		1328	50	0.85
Beech wood char	(in fluid bed combustor)	0.85		898-1223	51	0.85
Biomass char		0.85		1500		0.85
<b>Coal Particles</b>						
Devolatilising coal particle		0.6			56	0.6
Coal particle char	(0.9% ash)	0.8		400 - 900	1	0.81 - 0.79
Coal particle char				1473	56	0.83
Coal fly ash				500 - 1500	55,56,58-61	0.8-0.3
<b>Ash Particles</b>						
Coal ash	glassy	1	-40	500 - 1500	19	0.8-0.4
(deposited on furnace surfaces)	sintered	0.9	-30	500 - 1500	19	0.75-0.45
	powder, 120 $\mu$ m dia.	0.85	-30	500 - 1500	19	0.7-0.4
	powder, 33 $\mu$ m dia.	0.75	-30	500 - 1500	19	0.6-0.3
	powder, 6.5 $\mu$ m dia.	0.65	-30	500 - 1500	19	0.5-0.2
Wood ash	alkali-aluminosilicates	0.95	-30	500 - 1500	estimated	0.8-0.4

556

This paper is a compilation of radiant emissivity of high temperature materials.

Materials commonly used in furnaces such as metals and refractories are considered.

Data are given for fuels, chars and slags used in pf coal and biomass furnaces.